This full text paper was peer-reviewed at the direction of IEEE Instrumentation and Measurement Society prior to the acceptance and publication.

Smart Wall: Passive Visible Light Positioning with Ambient Light Only

Nathaniel Faulkner*, Fakhrul Alam*, Mathew Legg* and Serge Demidenko†*
*School of Engineering & Advanced Technology, Massey University, Private Bag 102904, Auckland, New Zealand
†School of Science & Technology, Sunway University, No.5 Jalan Universiti, Bandar Sunway, 47500 Selangor, Malaysia
Email: *{N.Faulkner, F.Alam, M.Legg, S.Demidenko}@Massey.ac.nz, †SDemidenko@Sunway.edu.my

***Abstract*—This paper reports the experimental results from a novel visible light positioning (VLP) system. The developed VLP is completely passive as it does not require the target to carry any active device or tag and, at the same time, it does not require any modification to the lighting infrastructure. The developed VLP localizes a target based on measuring the change it creates in the received signal strength (RSS) of the ambient light recorded at an array of photodiodes embedded in the wall. Experimental results from a prototype system show that a median error of 7.9 cm can be achieved.**

***Index Terms*—Indoor localization, Indoor Positioning System (IPS), Visible Light Positioning (VLP), Device Free Localization (DFL), Passive VLP**

I. Introduction

Indoor positioning has been a burgeoning area of research over the past decade. In terms of outdoor positioning, GPS [1] is the de facto solution, due to it being both ubiquitous and free to use. However, it has limitations, especially in built up areas or indoors [2]. The signal is negatively impacted by multipath reflections and struggles to penetrate walls. Furthermore, the offered accuracy of several metres [3] is not good enough for indoor applications. For these reasons, other methods have been proposed using infrared signals [4], RFID [5], Bluetooth [6] and Wi-Fi [7], [8]. Whilst most of these represent an improvement over GPS for indoor localization, the majority of them still do not meet the desired levels of accuracy, reliability or simplicity. With Light Emitting Diodes (LEDs) steadily replacing traditional lighting sources, a new method of positioning has come to the fore – Visible Light Positioning (VLP). Visible light has the benefits of being far less susceptible to multipath interference and flat fading due to its vastly higher frequency than RF [9]. LED lighting can also perform multiple roles – illumination, communication and positioning. Active VLP has been well researched and relies on a mobile object having a receiver containing either a photodiode or image sensor [10]. There are several active VLP methods that have been implemented on indoor testbeds, with the main approaches being Received Signal Strength (RSS) lateration [11]–[13], Angle of Arrival (AOA) angulation [14], [15], and fingerprint matching [16].

Passive VLP allows for the detection of people and objects without the need for the tracked object to have an attached receiving device. It is highly desirable to be able to track passively rather than relying on a wristband or other smart device which must be consciously put on. There are several existing works for passive VLP. In [17] the authors used co-located LED luminaires and photodiodes to passively detect humans. The light from the LED luminaires was multiplexed using Time-Division Multiple Access (TDMA) to identify the source of incoming light at each photodiode. In the aforementioned paper, the data was primarily used to detect whether a door was open or closed. The authors further extended this work in [18] to also track human movement and detect room occupancy. The authors were able to achieve 93.7% occupancy count accuracy and 0.89 m median error positioning accuracy in a 45 m^2 room. In [19], the floor is inlaid with 324 photodiodes, with 5 LED luminaires placed on the ceiling above. This setup is then used to detect the position of a human's body and limbs from the shadows cast onto the floor. The authors were able to achieve a mean angular accuracy of 10 degrees for the 5 main body joints. The work was further extended in [20] using only 20 photodiodes, albeit with a much larger number of LED panels on the ceiling. This simplifies the infrastructure at the cost of slightly decreased accuracy – 13.6 degrees mean angular error instead of 10. Similarly, the authors in [21] also use a grid of photodiodes embedded into the floor. LED luminaires on the roof cast shadows from test subjects onto said photodiodes. However, this paper reports results based on mostly simulation, with the only experimental part being a single point to point LED to photodiode link to gather parameters for the larger scale simulation. In simulations, the authors were able to achieve median error of 8cm in an 8m x 8m x 4m room with 4 LED luminaires, and photodiodes uniformly spaced at 0.5m in the floor. In [22], the authors use a passive VLP approach for mobile device input using an LED and two photodiodes to detect a user's finger. The LED improves the reliability in the presence of changing ambient light. The authors were able to position a user's finger in a 9x7 cm grid with 0.7 cm median error. CeilingSee [23] uses reverse biased LED luminaires as photodiodes for occupancy sensing. However, the authors did not use the system for positioning of test subjects or objects and therefore, do not have a position accuracy.

This paper, focuses on achieving accurate positioning of an object in ambient light conditions without the need of any modification to the existing lighting, unlike the majority of

This research was supported by the Massey University Research Fund (MURF) 2017-18 "Implementation of an Asset Tracking & Monitoring System Leveraging Existing Wi-Fi & Lighting Infrastructure"

978-1-5386-3460-8/19/$31.00 ©2019 IEEE

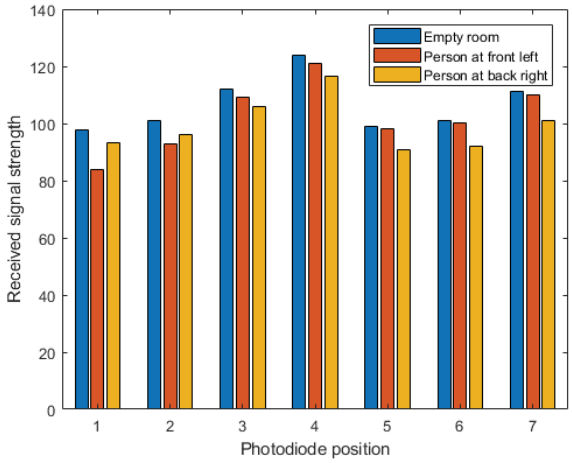

Fig. 1. Received power at each photodiode for three scenarios - empty test bed, test subject at left hand side close to the wall with the photodiodes affixed, and right hand side away from wall with photodiodes affixed. Corridor environment

VLP solutions.

II. System overview

In a room, there are generally multiple light sources – several interior lights and in many cases, windows as well. In addition to this, walls are generally light coloured and, therefore, cause a portion of the light to be reflected. A person moving around a room produces several shadows of different intensities to be projected onto the floor and walls. The main shadows comes from blocking the direct path from the ambient light sources. However, many other shadows are generated because the reflected components from the light sources are also blocked. These shadows can be detected by photodiodes placed around a room and then used to locate objects. This can be observed in Fig. 1. The blue bars are the RSS at seven different photodiodes placed along a wall when the test area is free from obstructions. The red and orange bars present a case when a person is standing at the front left (close to the wall) and the back right (further from the wall) respectively. This causes RSS to drop compared to the empty room, with there being a greater drop at photodiodes closer to the test subject. For example, when the test subject is in the front left position, the RSS drop is more significant in photodiodes 1 and 2 and there is very little drop in photodiodes 6 and 7. When the person is at the back right, the opposite is true - photodiodes 6 and 7 are affected to a much larger degree than 1 and 2.

The testbed makes use of seven ISL29023 [24] integrated digital light sensors placed on a board (wall) at a height of 1.05 meters from the floor. The light sensors are comprised of a photodiode, transimpedance amplifier, and analog-to-digital converter (ADC) located on the same package. Each light sensor is connected to a low-cost Wi-Fi microchip (ESP8266 [25]) as shown in Fig. 2. The ambient light manifests as DC at the output of the transimpedance amplifier. The DC level is

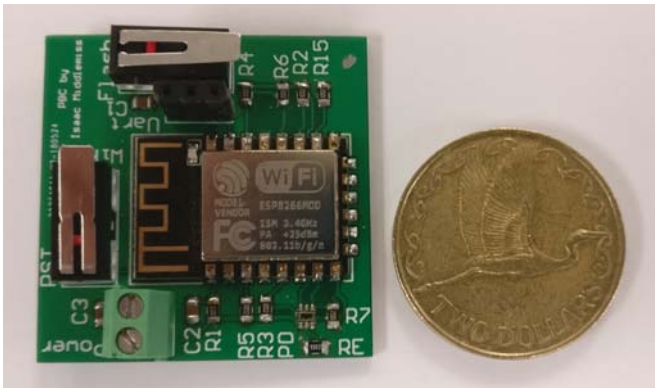

Fig. 2. Photodiode receiver.

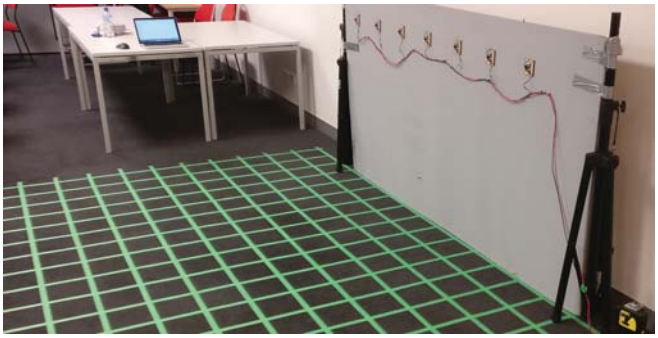

Fig. 3. Smart wall with the embedded photodiode receivers, open room environment.

a measure of the RSS of the ambient light and is sampled by the embedded ADC and is retrieved by the microcontroller in the ESP8266. The latest 100 samples are stored in the memory until they are retrieved over Wi-Fi. The data can then be requested in 100 value packets from a laptop and saved to the hard drive.

A 3.4m x 2.2m grid with 20cm squares was marked out using masking tape and a laser straight edge.

Two experiments were performed, one with the photodiodes along the wall facing into the room – henceforth known as the open room environment (see Fig. 3). For the second experiment, the photodiodes were positioned along the side of the grid furthest from the wall, with the photodiodes pointing back towards the wall – henceforth known as the corridor environment (see Fig. 4). Immediately before and after each test, the background ambient light measured and recorded. This was then used to normalise the data at each photodiode and verify the ambient light levels remained constant - a factor which this work is reliant on. Changes in ambient light would introduce extra uncertainty and consequently decreased positioning accuracy. Each measurement consists of 100 RSS readings over 10 seconds at each photodiode. This could potentially be reduced (or the data sample rate increased) in later works to hasten the data acquisition process.

Data were collected at each grid intersection for a total of 198 locations, with the data being split into two parts with

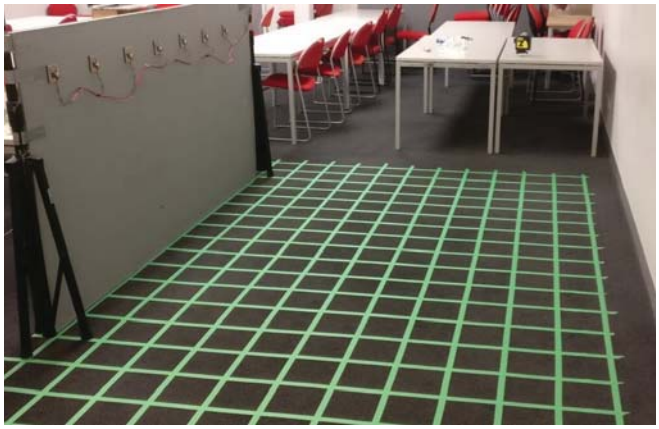

Fig. 4. Smart wall with the embedded photodiodes, corridor environment.

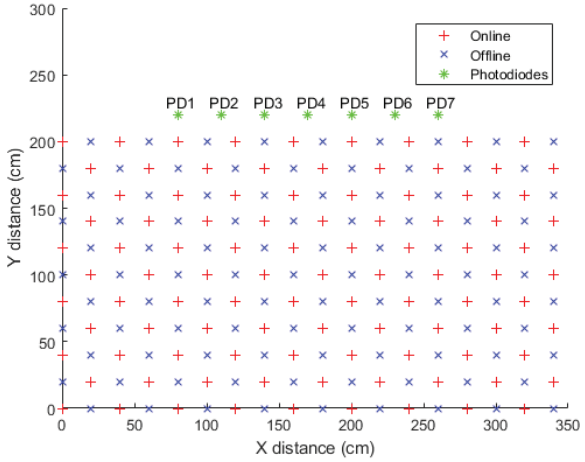

Fig. 5. Online vs offline data points.

half forming the offline fingerprint database, and the other half, the online RSS measurements. The online and the offline locations are shown in Fig. 5. The measured RSS values at each photodiode are shown in Fig. 6. These plots show the change in RSS with a test subject (180 cm in height) standing at each individual point on the grid - combining both the online and offline points. A very large dip can be seen on the top left edge of each plot where the test subject stood immediately in front of the photodiode causing a strong shadow. Taking the RSS value from the same location on each plot gives the fingerprint value for that position. Weighted K Nearest Neighbours (WKNN) [26] was employed to classify the online readings using the offline fingerprints. Euclidean distance was used to measure the distance between the online reading and each entry on the fingerprint database.

A. WKNN algorithm

Weighted K nearest neighbours is an extension of the K nearest neighbours algorithm [27]. The algorithm takes a live reading R_{live} which is a vector of M RSS readings - one from each photodiode. This is compared to the offline fingerprint database R which stores a vector R for each point that has been mapped. The Euclidean distance d_i between R_{live} and an entry in the database $R_{i,j}$ is taken as follows:

$$d_i = \sqrt{\sum_{j=1}^{M}(R_{i,j}^2 - R_{live}^2)} \tag{1}$$

The K smallest distance entries in the database are taken and used to estimate the weights for each of the K database readings as:

$$W_k = \frac{1}{d_k} \tag{2}$$

These are then used to weight each of the locations before they are combined. This is so that the database readings closest to the live reading have a greater influence on the final position estimation. The final position is found as follows:

$$\widetilde{x}_j = \frac{\sum_{k=1}^{K} W_{j,k} \times x_k}{\sum_{k=1}^{K} W_{j,k}} \tag{3}$$

$$\widetilde{y}_j = \frac{\sum_{k=1}^{K} W_{j,k} \times y_k}{\sum_{k=1}^{K} W_{j,k}} \tag{4}$$

Where $[\widetilde{x}_j, \widetilde{y}_j]$ is the estimated position, $W_{j,k}$ are the weights calculated in equation (2) and $[x_k, y_k]$ is the associated coordinate for that weight. The position error is then calculated by finding the Euclidean distance between the estimated location and the actual location where the live RSS values were taken.

III. Experimental Results

A K value of 3 was experimentally chosen for the WKNN algorithm, as it provides a good balance between optimising both the median and maximum error for both environments. This can be clearly seen in Fig. 7.

TABLE I
Position error for K = 3 for both environments

	Corridor	**Open room**
Median error (cm)	7.9	12.3
Max error (cm)	97	357
Standard deviation (cm)	14.3	40.8

Table I shows the position errors for both the experiments. In Fig. 8, the estimated positions for the corridor are plotted in relation to their actual locations to show the spatial error distribution. One can see that the errors are concentrated at the boundaries of the testbed. In part, this is due to the positions being further from the photodiodes and in part, due to having less fingerprints around the position. Fig. 9 shows the localization errors for the open room environment. As expected from the Cumulative Distribution Function (CDF) plot in Fig. 10, one can see that the position estimation is

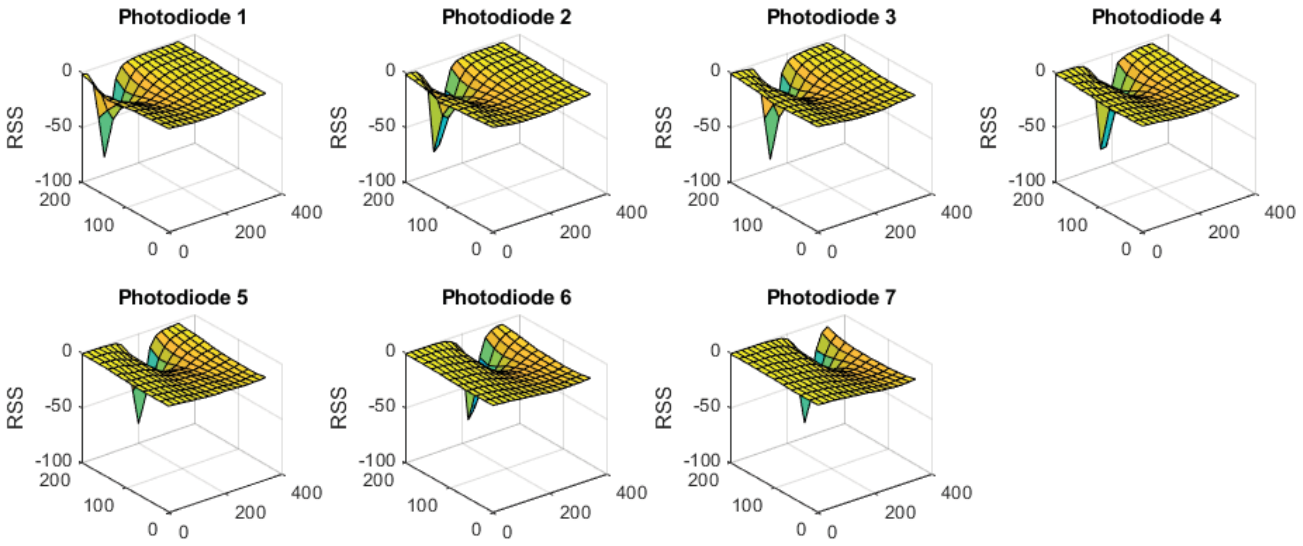

Fig. 6. RSS fingerprints for each photodiode. Corridor environment.

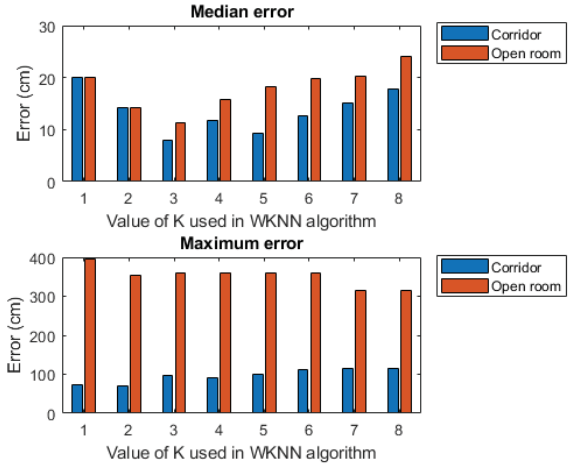

Fig. 7. The impact of the value of K on both the median and maximum error for both the environments (corridor and open room).

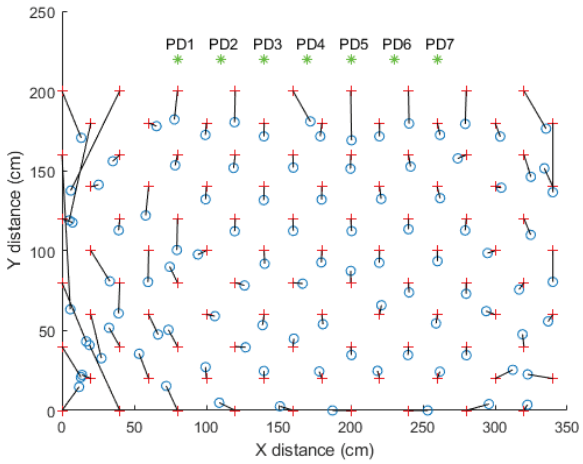

Fig. 8. Actual vs estimated positions in the corridor environment. Green asterisks denote the photodiode positions, red crosses the actual positions, the blue circles the estimated positions and the black lines the magnitude of the error between the actual and estimated positions.

more accurate for the corridor environment. It is more accurate due to the light reflecting off the white wall behind causing more distinct shadows. The worst case errors in the open room scenario are at the very edges of the testbed. In particular, the two corners closest to the photodiode wall which are at a very acute angle to the majority of the photodiodes and, therefore, do not experience a discernible shadow. This can be seen in Fig. 11 where the two corner RSS plots are compared to the background RSS reading and also a position with low error. The RSS readings at the two corner plots are both very similar to the background readings. They are most different at photodiode 1 for the left hand reading and photodiode 7 for the right hand reading as these are the least acute angles. As the RSS readings are so close to the background readings, small amounts of noise can cause erroneous identification of neighbours leading to large errors in the position estimate. This can be addressed by extending the row of the photodiodes further along the wall.

IV. Conclusion

The authors believe that this is the first reported passive VLP reported in the literature that uses only the ambient light. The system is able to position an object with a median error of 7.9cm in a corridor environment. In an open room scenario, this increases to 11.4 cm median error. Further work should

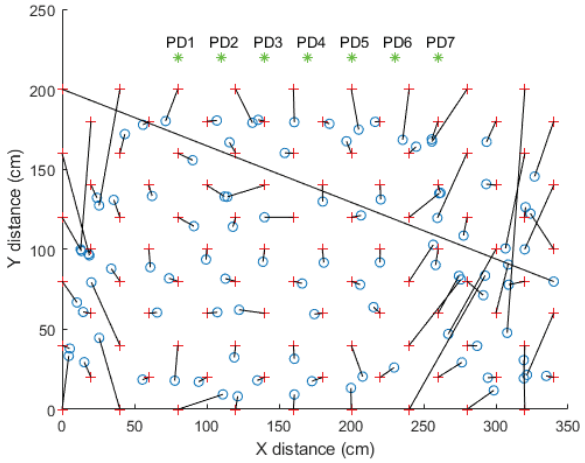

Fig. 9. Actual vs estimated positions in the open room environment. Green asterisks denote the photodiode positions, red crosses the actual positions, the blue circles the estimated positions and the black lines the magnitude of the error between the actual and estimated positions.

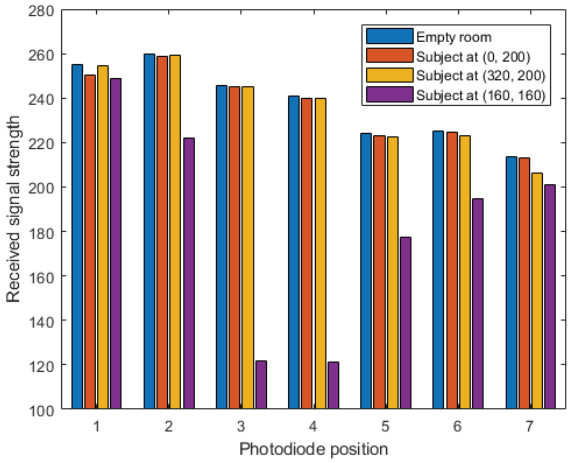

Fig. 11. The worst errors are found at (0, 200), (320, 200). This is compared to a location with a much lower error at (160, 160) and the readings when no test subject is present. Open room environment

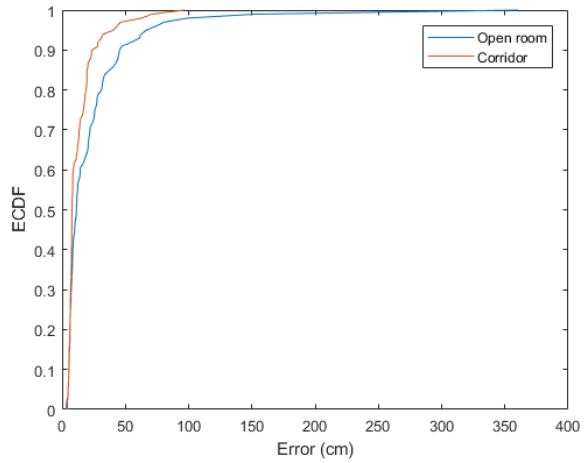

Fig. 10. Localization precision as CDF of error in both environments.

expand the test to a full room scale. The experiments were undertaken at night and, therefore changes in the level of ambient light was not investigated. This is the area for future investigations to quantify and potentially mitigate the impact it may have. Modulated light could potentially be used from LED ceiling luminaires to mitigate the effect of ambient light. Currently the system has been tested for a single object at a time and as such, further investigation is needed to detect multiple objects. With fingerprint based systems, generating the fingerprint database is a very time consuming process. In the future, the authors will investigate how to model these data and generate them from a few strategically selected calibration points.

ACKNOWLEDGMENT

The authors would like to acknowledge Isaac Middlemiss for his help developing the hardware and for his assistance in conducting some preliminary experiments.

REFERENCES

[1] J. Farrell and M. Barth, *The global positioning system and inertial navigation*, vol. 61. Mcgraw-hill New York, 1999.

[2] M. B. Kjærgaard, H. Blunck, T. Godsk, T. Toftkjær, D. L. Christensen, and K. Grønbæk, "Indoor positioning using GPS revisited," in *International conference on pervasive computing*, Springer, 2010.

[3] M. G. Wing, A. Eklund, and L. D. Kellogg, "Consumer-grade global positioning system (gps) accuracy and reliability," *Journal of forestry*, vol. 103, no. 4, p. 169, 2005.

[4] R. Want, A. Hopper, V. Falcao, and J. Gibbons, "The active badge location system," *ACM Transactions on Information Systems (TOIS)*, vol. 10, pp. 91–102, 1992.

[5] L. M. Ni, Y. Liu, Y. C. Lau, and A. P. Patil, "LANDMARC: indoor location sensing using active RFID," in *Proceedings of the First IEEE International Conference on Pervasive Computing and Communications*, IEEE, 2003.

[6] A. Kotanen, M. Hannikainen, H. Leppakoski, and T. D. Hamalainen, "Experiments on local positioning with Bluetooth," in *Information technology: Coding and computing [computers and communications], 2003. Proceedings. ITCC 2003. International conference on*, IEEE, 2003.

[7] M. Youssef and A. Agrawala, "The Horus WLAN location determination system," in *Proceedings of the 3rd international conference on Mobile systems, applications, and services*, ACM, 2005.

[8] P. Bahl and V. N. Padmanabhan, "RADAR: An in-building RF-based user location and tracking system," in *INFOCOM 2000. Nineteenth Annual Joint Conference of the IEEE Computer and Communications Societies. Proceedings. IEEE*, Ieee, 2000.

[9] T. Komine and M. Nakagawa, "Fundamental analysis for visible-light communication system using LED lights," *IEEE transactions on Consumer Electronics*, vol. 50, pp. 100–107, 2004.

[10] W. Zhang and M. Kavehrad, "Comparison of VLC-based indoor positioning techniques," in *Broadband Access Communication Technologies VII*, International Society for Optics and Photonics, 2013.

[11] P. Hu, L. Li, C. Peng, G. Shen, and F. Zhao, "Pharos: Enable physical analytics through visible light based indoor localization," in *Proceedings of the Twelfth ACM Workshop on Hot Topics in Networks*, ACM, 2013.

[12] B. Xie, K. Chen, G. Tan, M. Lu, Y. Liu, J. Wu, and T. He, "LIPS: A light intensity–based positioning system for indoor environments," *ACM Transactions on Sensor Networks (TOSN)*, vol. 12, p. 28, 2016.

[13] D. Konings, B. Parr, F. Alam, and E. M. Lai, "Falcon: Fused application of light based positioning coupled with onboard network localization," *IEEE Access*, vol. 6, pp. 36155–36167, 2018.
[14] Y.-S. Kuo, P. Pannuto, K.-J. Hsiao, and P. Dutta, "Luxapose: Indoor positioning with mobile phones and visible light," in *Proceedings of the 20th annual international conference on Mobile computing and networking*, ACM, 2014.
[15] M. Yasir, S.-W. Ho, and B. N. Vellambi, "Indoor position tracking using multiple optical receivers," *Journal of Lightwave Technology*, vol. 34, no. 4, pp. 1166–1176, 2016.
[16] F. Alam, M. T. Chew, T. Wenge, and G. S. Gupta, "An accurate visible light positioning system using regenerated fingerprint database based on calibrated propagation model," *IEEE Transactions on Instrumentation and Measurement*, 2018.
[17] M. Ibrahim, V. Nguyen, S. Rupavatharam, M. Jawahar, M. Gruteser, and R. Howard, "Visible light based activity sensing using ceiling photosensors," in *Proceedings of the 3rd Workshop on Visible Light Communication Systems*, ACM, 2016.
[18] V. Nguyen, M. Ibrahim, S. Rupavatharam, M. Jawahar, M. Gruteser, and R. Howard, "Eyelight: Light-and-shadow-based occupancy estimation and room activity recognition," in *IEEE INFOCOM 2018-IEEE Conference on Computer Communications*, IEEE, 2018.
[19] T. Li, C. An, Z. Tian, A. T. Campbell, and X. Zhou, "Human sensing using visible light communication," in *Proceedings of the 21st Annual International Conference on Mobile Computing and Networking*, ACM, 2015.
[20] T. Li, Q. Liu, and X. Zhou, "Practical human sensing in the light," in *Proceedings of the 14th Annual International Conference on Mobile Systems, Applications, and Services*, ACM, 2016.
[21] S. Zhang, K. Liu, Y. Ma, X. Huang, X. Gong, and Y. Zhang, "An accurate geometrical multi-target device-free localization method using light sensors," *IEEE Sensors Journal*, vol. 18, no. 18, pp. 7619–7632, 2018.
[22] C. Zhang, J. Tabor, J. Zhang, and X. Zhang, "Extending mobile interaction through near-field visible light sensing," in *Proceedings of the 21st Annual International Conference on Mobile Computing and Networking*, ACM, 2015.
[23] Y. Yang, J. Hao, J. Luo, and S. J. Pan, "CeilingSee: Device-free occupancy inference through lighting infrastructure based LED sensing," in *IEEE International Conference on Pervasive Computing and Communications (PerCom), 2017*, IEEE, 2017.
[24] Renesas, *ISL29023 Integrated Digital Light Sensor with Interrupt*, May 2014. Rev. 4.
[25] Espressif Systems, *ESP8266EX Datasheet*, November 2018. Rev. 6.
[26] S. A. Dudani, "The distance-weighted k-nearest-neighbor rule," *IEEE Transactions on Systems, Man, and Cybernetics*, no. 4, pp. 325–327, 1976.
[27] N. S. Altman, "An introduction to kernel and nearest-neighbor nonparametric regression," *The American Statistician*, vol. 46, no. 3, pp. 175–185, 1992.